Journal of Power Sources 204 (2012) 100–105

Contents lists available at SciVerse ScienceDirect

Journal of Power Sources

journal homepage: www.elsevier.com/locate/jpowsour

Analysis of the thermal field of a seal-less planar solid oxide fuel cell

P. Leone[a,*], A. Lanzini[a], B. Delhomme[a], G.A. Ortigoza-Villalba[a], F. Smeacetto[b], M. Santarelli[a]

[a] Dipartimento di Energetica, Politecnico di Torino - Corso Duca degli Abruzzi 24, 10129 Torino, Italy
[b] Dipartimento di Scienza dei Materiali e Ingegneria Chimica, Politecnico di Torino - Corso Duca degli Abruzzi 24, 10129 Torino, Italy

ARTICLE INFO

Article history:
Received 6 October 2011
Received in revised form
24 November 2011
Accepted 6 December 2011
Available online 13 December 2011

Keywords:
Experimental
Solid oxide fuel cells
Temperature measurements
Thermal gradients
Fuel mixtures

ABSTRACT

This work focuses on the thermal behavior of an anode-supported planar solid oxide fuel cell (SOFC) running under different operating conditions and fuel compositions. A seal-less in-house ceramic housing was specifically designed and built to test the fuel cells and characterize their electrical performance as well as the thermal field established across the anode surface area. The housing design we used allowed us to measure the temperature in 8 different positions along the cell radius. Our experimental sessions were thus dedicated to observe the electrochemical performance and the established temperature field across the SOFC active area under several operating conditions, obtained by varying the inlet fuel composition, the fuel utilization factor and the current density, respectively. The fuel composition was varied by feeding the SOFC with hydrogen fuel, diluted-hydrogen and finally methane, in a direct internal steam reforming configuration. During each experiment, the temperature field across the cell was measured while varying the current density; results were compared together among the different fuel compositions used, showing a consistent thermal gradient established even with relatively small-sized cells. The paper also outlines key issues in the development of ceramic housings with multi-measurement capability.

1. Introduction

Solid oxide fuel cells are expected to reach further reliability over the next few years and enter the market with satisfactory life-time requirements and performance. Among the key issues needed to meet the required technical and performance targets (from which economic aspects will take advantage as a consequence), understanding the SOFC thermal behavior under relevant operating conditions is certainly useful. Degradation phenomena of SOFC materials are generally enhanced by temperature hot spots or temperature gradients [1–4] within the fuel cell; on the other side, cold spots drastically reduce the local cell performance and can be responsible of a disuniformity of the current generation profile over the cell's active surface area. Especially when operating the SOFC in a direct internal reforming configuration (which is probably one of the key technical features to meet high efficiency at low system costs), strong thermal gradient across the cell and, more widely, across the stack structure can be produced.

The thermal behavior of SOFCs has been not studied steadily by the research community; in the literature, most of the research works address this topic with CFD modeling tools, without including an adequate validation of their simulations [5–10]. There are only few experimental studies [11–16] dealing with thermal behavior of SOFC, nonetheless related with a button cell test set-up (i.e. with an active area which is an order of magnitude smaller than the size used in this paper).

Adzic et al. [11] proposed dedicated instrumentation for temperature measurements in an SOFC; the authors determined the right dimensions for thermocouples to avoid as much as possible errors deriving from the radiative and convective heat transfer, respectively.

In [12], Morel et al. show how the measurement of the ohmic resistance of thick electrolyte cells provides excellent results to evaluate the temperature gradients.

More recently, Brett et al. [14] used infra-red (IR) imaging techniques to measure the temperature field over an SOFC surface; they found that for a button cell (1 cm^2 active area) the temperature is not completely uniform and can be a source for error in the evaluation of some kinetic parameters. Also Larrain et al. [16] have shown that a temperature gradient can occur at high current density even in button cell test configurations.

As far as it concerns cells with a wider area, we are not aware of dedicated experimental studies. In our study presented here, a method to easily measure temperature gradients of an SOFC along the gas distribution channels is proposed and results are presented concerning with a wide range of SOFC operating conditions.

* Corresponding author.
E-mail address: pierluigi.leone@polito.it (P. Leone).

0378-7753/$ – see front matter © 2011 Elsevier B.V. All rights reserved.
doi:10.1016/j.jpowsour.2011.12.004

2. Experimental

The experiments were carried out in a test-rig consisting for high temperature characterization of SOFC cells. The fuel cell is contained in an electrically heated furnace; both electrodes contact with a ceramic housing; each housing is responsible for (i) distributing either the anodic or the cathodic reactant gas over the electrode's active surface, and (ii) providing electrical connection between the electrode and an external electric circuit.

The cathodic housing employed consisted of a sintered alumina block having the side contacting the electrode finely machined to provide gas channels able to adequately distribute the gas over the whole active area; a Pt current collecting mesh along with Pt leads were included to provide a good electrical contact between the cell and the external electric circuit. The anode housing was specifically designed to perform temperature measurements in proximity of the electrode's surface; it consisted of an alumina block that was machined on the contacting the electrode to ensure both a proper fuel distribution as well as to provide the location for the placement of various thermocouples. A Ni current collecting mesh along with Pt current leads were included to provide a good electrical contact between the cell and the external electric circuit.

Both anode and cathode housings were machined by providing an array of parallelepiped type separators with edge of 1.5 mm and height of 0.5 mm aiming to ensure a proper distribution of reactants over the cell active surface.

The test-stand also included a gas supply system with mass flow controllers (Bronkhorst, The Netherlands) for CH_4, H_2, N_2, CO and CO_2 (anode side) and a bubbler to provide proper humidification to the inlet dry gas; an air compressor (with filter and dehumidifier) connected to an air mass flow controller was used to feed the cathode side. Concerning the electrical/electrochemical measurements, the test-stand was also equipped with an electronic load (Kikusui Electronics Corp., Japan) in conjunction with an additional power supply operating in current-following mode (Delta Elektronica, The Netherlands) for current–voltage measurements and a Gamry FC350 impedance analyzer to measure the impedance frequency response of the cell between 1 mHz and 300 kHz.

The experiments were carried out on a circular anode supported cell 80 mm in diameter, made of a 500 μm Ni/8YSZ porous anode support, a 10 μm denser Ni/8YSZ anode active layer, a 5 μm fully dense 8YSZ electrolyte and LSM/8YSZ double cathode layer (15 μm LSM/8YSZ active layer plus 20 μm of pure LSM porous current collector layer). Further details on cell geometry and materials have been previously reported [17,18].

The experiments were performed fixing the oven temperature at 800 °C, while providing the fuel cell with different anode feeds, including hydrogen, nitrogen-diluted hydrogen and methane with steam addition to promote direct internal steam reforming while avoiding carbon deposition. The summary of performed experiments is given in Table 1.

3. Multi-measurements housing development

As briefly introduced before, a ceramic housing was specifically designed and machined to perform temperature measurements within a planar SOFC. Two fundamental issues were addressed concerning the optimization of the electrical contacts between the electrode and the external circuit and the placement and sealing of thermocouples inside the gas channels to measure the temperature profile along the radius of the SOFC.

For SOFC testing purposes, the minimization of external contact resistances (which account for parasitic ohmic losses and thus would lead to an over-estimation of the cell resistance) is important; often, metallic meshes are used to guarantee a proper electrons' transfer between the electrodes and some external circuit. In our anodic housing design, we adopted a solution in which the electrical contact between the mesh (made of Nickel) and the current leads (made of Platinum) to the external circuit was provided by a heat treatment in vacuum atmosphere that permitted us to join Pt–Ni samples by solid state diffusion bonding. Such thermally enhanced joining procedure was carried out at 1100 °C with a dwelling time of 6 h (and a heating rate of 10 °C min^{-1} and a cooling rate of 5 °C min^{-1} were used). The heat treatment was performed in vacuum atmosphere at 10^{-2} mbar. The Pt–Ni joined structures were observed with FE-SEM (FEI Inspect, Philips 525) and analysed with EDS (SW9100 EDAX) revealing the occurred atomic inter-diffusion of nickel and platinum, respectively.

An overall of 9 K-type thermocouples were placed in the anodic housing, as shown is Fig. 1, in order to perform the temperature measurements; each thermocouple was 1 mm in diameter each and was inserted through a hole drilled directly in the ceramic housing between the different channels distributing the fuel. The head (sensing part) of the thermocouple reached the bottom surface of the gas channel: with such arrangement, the distance between the anode electrode and the thermocouple was equal to the channel height (i.e. 0.5 mm). The location (in polar coordinates) of the thermocouples within the fuel cell is shown in Fig. 1. To avoid gas leakage through the drilled holes, a high temperature ceramic adhesive Aremco Ceramabond 516 was used.

The thermocouples were all calibrated in oven over a temperature ranging from 750 to 850 °C prior of conducting the experiments; the maximum observed temperature variation observed from one thermocouple to another was 1.4 °C.

At the cathode side, a commercial ceramic housing (ECN, The Netherlands) was used, with Pt wires and Pt mesh for the current collection contacted together by spot-welding.

4. Experimental results

4.1. Electrochemical measurements

The anode housing designed to have multiple temperature measurements in the gas channels provided results comparable with those achieved by using commercial testing housing without holes drilled for placing thermocouples. Also, the measured ohmic resistance of the tested cells was not affected by the heat-assisted welding procedure between Pt current leads and Ni mesh that we developed [17]. Only we found open circuit voltages that were a bit lower than we expected (around 50 mV lower) probably due to some fuel leaking from the thermocouples' holes.

Fig. 2 shows the polarization curves for the SOFC fed by hydrogen at different fuel utilizations. The operation at high fuel utilization (FU) is required to achieve high efficiencies; however, the higher the fuel utilization, the higher will be the overpotentials generated within the cell due to the lower partial pressure of reactant gases at the anode's three phase boundary (TPB).

In general, the higher is the current drawn by fuel cell (and consequently the FU, if a constant anode feed is maintained as we did while measuring the current–voltage traces) the more pronounced is expected to be the impact over the cell's thermal field.

Fig. 3 shows the polarization curves of a planar SOFC fed by nitrogen-diluted hydrogen mixtures with different dilution percentages. The dilution with nitrogen does not affect heavily the fuel cell operation at low and medium current densities, whereas produces mass transport limitations at high current density.

Fig. 4 shows the polarization curves measured under direct methane steam reforming at different steam-to-fuel molar ratios.

Table 1
Experimental flow conditions employed during the experiments.

Test number	Fuel (Nml min^{-1})						
	H_2	N_2	CO_2	CO	CH_4	H_2O	FU @ 0.5 A cm^{-2}
1	250	0	0	0	0	10.25	66
2	500	0	0	0	0	20.5	33
3	1000	0	0	0	0	41	16.5
4	500	500	0	0	0	41	33
5	500	300	0	0	0	32.8	33
6	500	100	0	0	0	24.6	33
7	0	0	0	0	125	375	33
8	0	0	0	0	125	250	33
9	0	0	0	0	125	187.5	33

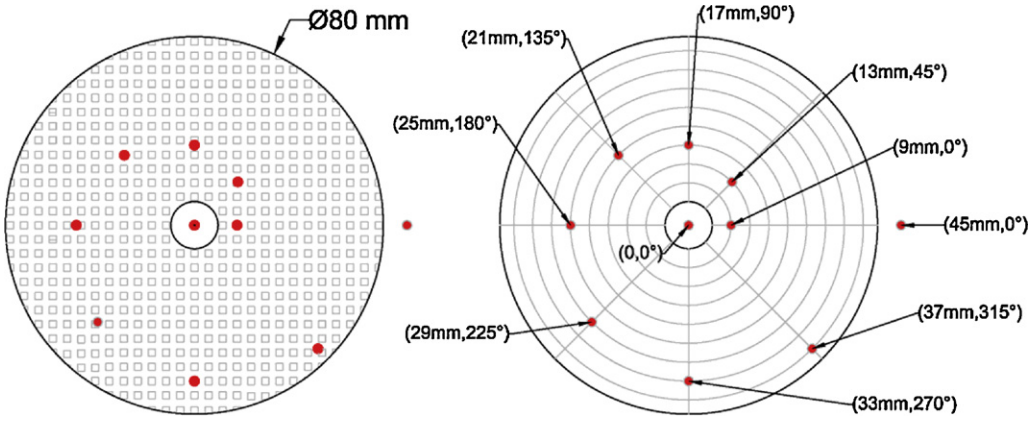

Fig. 1. Schematic of the ceramic test housing with spots for temperature measurements.

The cell performance is slightly lower than the cases with hydrogen, essentially due to the lower Nernst voltage achieved. The effect of steam addition produces negative effects (lowering the voltage) especially at the higher current densities, again due mass transfer limitations effects (i.e. an enhanced difficulty for the fuel gas to flow through the porous anode support and finally reach to reach the TPB active sites).

The cell performance observed in Figs. 2–4 will be used to discuss its thermal behavior, introduced in next paragraph.

4.2. Temperature measurements

In Fig. 5, the effect of hydrogen flow on the radial thermal profile of the cell is shown (experiments 1–3 referring to Table 1).

At low current density, both cell polarization and fuel utilization are pretty low, therefore a very small amount of heat is generated by the electrochemical reactions and ohmic losses, and so a rather flat temperature profile is observed that is only slightly affected by

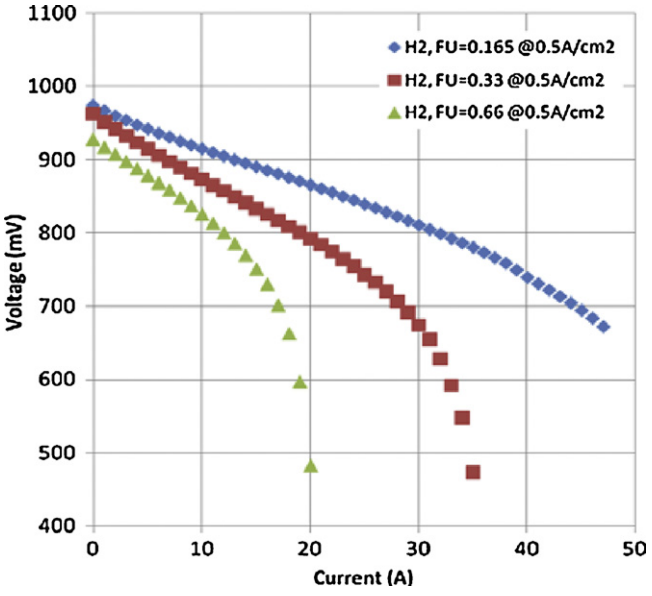

Fig. 2. Polarization curves of the SOFC with H_2 fuel.

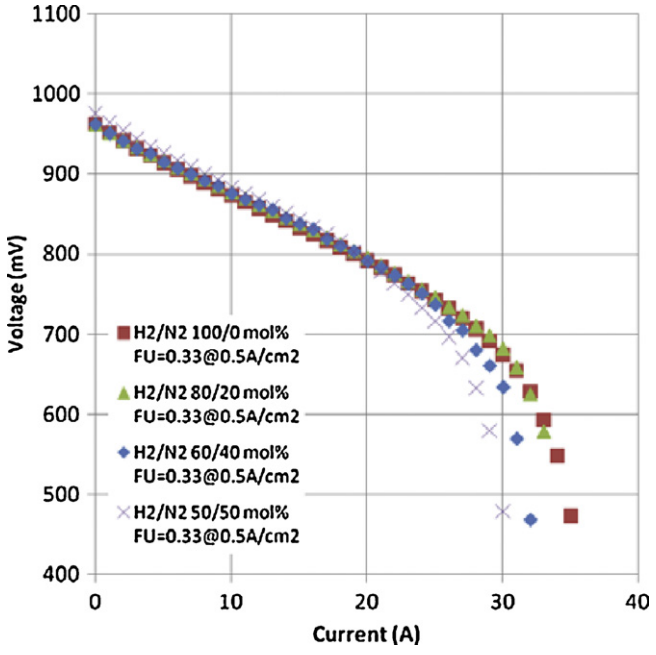

Fig. 3. Polarization curves fuelled of the SOFC with H_2/N_2 mixtures.

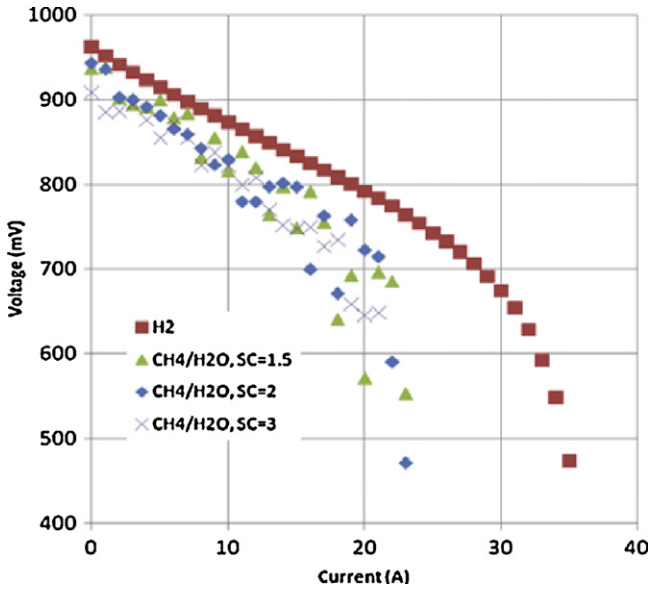

Fig. 4. Polarization curve of the SOFC with CH_4/H_2O mixtures.

the cell' operating conditions. Concerning the high temperatures reached at the outer zone of the cell, combustion of the anode off-gas with air must occur there due to an air backflow.

As the operating current increases, the temperature profile becomes more complex in shape, featuring two local maxima; the first one lies within the first 10 mm of the cell's radius, and can be attributed to the cell's operation (i.e. the sum of the heat of reaction plus the heat due to irreversibilities); the second maximum lies instead in the outer border region of the fuel cell, and is attributed to combustion phenomena already described.

About the first local maximum, it becomes such only when the cell's overvoltage increases above a certain threshold ($\Delta V > 150$ mV), with a trend pretty much identical for all flow conditions shown in Fig. 5, which suggests that the current density profile along the cell radius also reaches a maximum at $r = 10$ mm; in fact, as the current density increases, the cell polarization increases as well and a larger amount of heat is generated by the cell. The occurring of the first local temperature hot spot at the specific location of $r = 10$ mm is attributed due to a combination of several factors depending on the reactants' distribution configuration (at both the anode and cathode sides), and the current operating condition. In particular, it is reasonable to establish a link between the cell's temperature gradient along the radial coordinate to and the local distribution of current density along the same direction. In particular, a proper design of distribution channels for the reactant gases could lead to a homogenization of the current distribution, thus leading to smoother temperature gradients.

In general, when the total cell current increases the temperature profile results strongly affected by the cell operating conditions and a larger temperature gradient across the gas channels is observed; among the three different fuel flow conditions investigated (250, 500, 1000 Nml min^{-1} of H_2 flow, respectively), the temperature variation at 10 mm from the fuel inlet (i.e. the locus of the first temperature maximum) ranges from 20 °C to 40 °C. Concerning the second temperature maximum (due to combustion of the anode off-gas), the peak becomes pronounced as the total H_2 flow increases, confirming once again that combustion actually takes place at the cell's border region. As the current increases, the FU increases as well and a minor amount of fuel is left to burn; as a consequence, more air is able to diffuse toward the anode compartment, which eventually burn with hydrogen in a inner region of the anode; this is the reason why the second local temperature peak is actually observed only for FUs above a certain threshold (FU > 30%). For lower FUs, the peak of temperature occurs outside the cell, in the oven's volume immediately surrounding the cell. Further temperature measurements taken just outside the cell in the oven volume (also shown in the Fig. 1) – at 0.5 cm from the cell (and housing) outer border – confirm that the peak temperature reached due to combustion phenomena occurs either inside the anodic gas channel and in the outer annular region of the fuel cell depending on the fuel utilization operating conditions.

In Fig. 6, the effect of nitrogen dilution over the radial thermal profile of the fuel cell is shown. The trends observed are similar to those discussed before in case of pure hydrogen feeding.

The dilution with up to 50 mol.% of N_2 does not lead to significant additional polarization losses (as shown in Fig. 3); as a direct consequence, no further heat is generated by irreversibilities compared to the pure H_2 feed case. Nonetheless, a decrease of the cell average temperature and smoother thermal gradients are observed due to the higher convective flow of the inlet fuel (whose mass flow resulted significantly increased by the mixing of H_2 with N_2). Also, the dilution with nitrogen leads to a slight decrease of the combustion temperature essentially for the same reasons.

In Fig. 7, the effect of steam-to-carbon ratio over the radial thermal profile of a direct methane steam reforming SOFC is shown. The temperature profile along the radial coordinate is quite different with respect to the previous fuel compositions with H_2 fuel; the temperature at the cell inlet is 40–60 °C lower than with pure H_2 due to the endothermic reforming reactions of methane now occurring. Interestingly, there are no marked differences of temperature

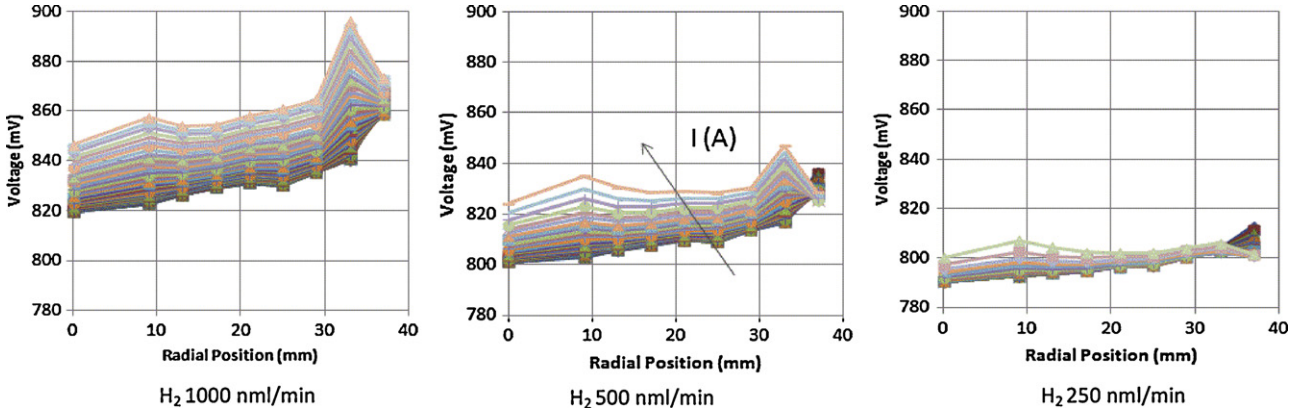

Fig. 5. Effect of hydrogen flow over the radial thermal profile of the SOFC.

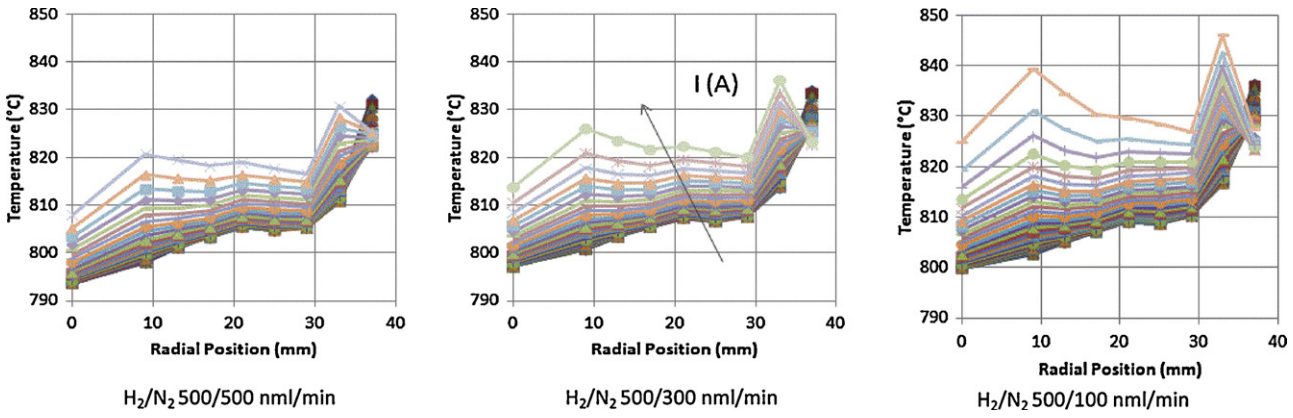

Fig. 6. Effect of nitrogen dilution over the radial thermal profile of the SOFC.

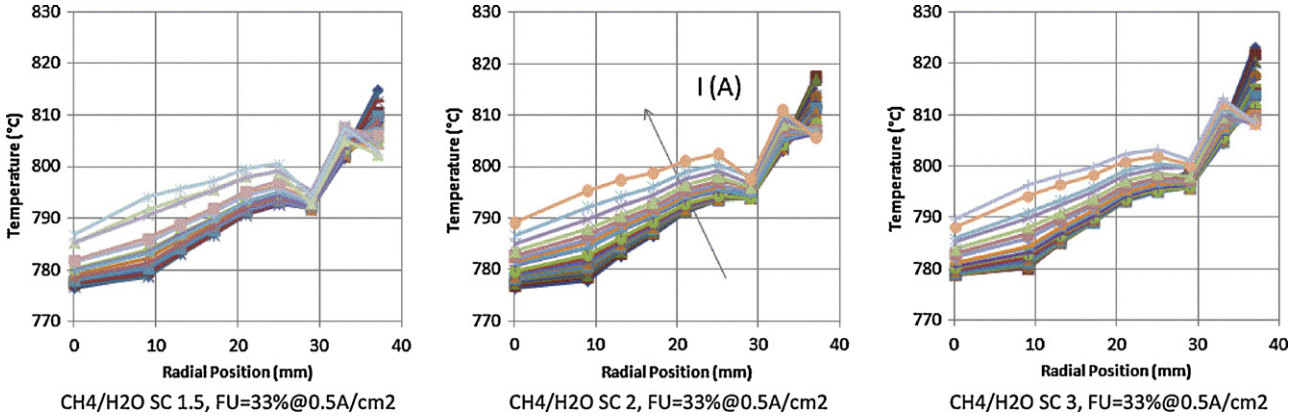

Fig. 7. Effect of the steam-to-carbon ratio over the radial thermal profile of a direct CH_4/H_2O fed SOFC.

profiles when varying the steam-to-carbon ratios. The temperature profile is again characterized by two local maxima, with the addition of local minimum in between. The first local maximum is still located in the inner region of the anode, but at a position much closer to the cell border than what previously observed with H_2 feeds; such peculiarity is attributed to the fact that endothermic reforming of methane retards the electrochemical reactions and the current density generation is more concentrated in the second half of the cell (whereas the first half acts more as a chemical reactor). The second maximum is again attributed to combustion reactions and qualitatively resembles the behavior already discussed for the previous fuel mixtures, even if combustion temperatures result generally lower with respect to previous cases because of the lower heating value of the reacting mixture.

5. Conclusions

The results shown provide a helpful insight about the importance of modeling assumptions (e.g. isothermal vs. non isothermal modeling) when dealing with SOFC (even at the single cell scale) and the necessity of thermal models validation with multi-fuel feeds. In addition, our experimental methodology proved to be valuable tool for the identification of critical operating conditions leading to severe thermal gradients across the fuel cell. Our experimental method was also useful to evaluate indirectly and qualitatively the current distribution along the fuel channel. In the future, a sealed configuration could be even more practical to study the thermal behavior of SOFCs; in fact, such configuration would eliminate post-combustion phenomena of the anode off-gas at the cell border, resulting in a less biased and more accurate set of temperatures (from which to extrapolate through the use of inverse methods the current density profile of the fuel cell, for example).

Acknowledgements

This work has been developed in the framework of the two following projects: '*MULTI.S.S.*' (Multi fuelled SOFC stack) funded by the Piedmont Council and '*Sperimentazione e Analisi Energetica di celle SOFCs alimentate a Biogas per la Generazione di Energia*' funded by the Ministry for Education, University and Research (MIUR).

References

[1] A. Atkinson, B. Sun, Materials Science and Technology 23 (10) (2007) 1135–1143.
[2] D. Bronin, Proceedings of the Real SOFC Summer School, Varna Bugaria, September 2–7, 2007, 2007.
[3] K. Fischer, J.R. Seume, Journal of Fuel Cell Science and Technology 6 (1) (2009) 0110171–0110179.
[4] M. Santarelli, P. Leone, M. Calì, G. Orsello, Journal of Power Sources 171 (1) (2007) 155–168.
[5] B. Zitouni, G.M. Andreadis, B.M. Hocine, A. Hafsia, H. Djamel, Z. Mostefa, International Journal of Hydrogen Energy 36 (6) (2011) 4228–4235.
[6] H. Mahcene, H.B. Moussa, H. Bouguettaia, D. Bechki, S. Babay, M.S. Meftah, International Journal of Hydrogen Energy 36 (6) (2011) 4244–4252.
[7] T.X. Ho, P. Kosinski, A.C. Hoffmann, A. Vik, International Journal of Hydrogen Energy 35 (9) (2010) 4276–4284.
[8] I. Zinovik, D. Poulikakos, Electrochimica Acta 54 (26) (2009) 6234–6243.
[9] K. Fischer, J.R. Seume, Journal of Fuel Cell Science and Technology 6 (1) (2009) 0110021–01100211.
[10] M. García-Camprubí, H. Jasak, N. Fueyo, Journal of Power Sources 196 (17) (2011) 7290–7301.
[11] M. Adzic, M.V. Heitor, D. Santos, Journal of Applied Electrochemistry 27 (12) (1997) 1355–1361.
[12] B. Morel, R. Roberge, S. Savoie, T.W. Napporn, M. Meunier, Electrochemical and Solid-State Letters 10 (2) (2007) B31–B33.

[13] M.H. Wang, H. Guo, C.F. Ma, F. Ye, J. Yu, X. Liu, Y. Wang, C.Y. Wang, Fuel Cell Science, Engineering and Technology, 2003, pp. 95–100.
[14] D.J.L. Brett, P. Aguiar, R. Clague, A.J. Marquis, S. Schoöttl, R. Simpson, N.P. Brandon, Journal of Power Sources 166 (1) (2007) 112–119.
[15] M.B. Pomfret, D.A. Steinhurst, D.A. Kidwell, J.C. Owrutsky, Journal of Power Sources 195 (1) (2010) 257–262.
[16] D. Larrain, J. Van Herle, F. Maréchal, D. Favrat, Journal of Power Sources 118 (1–2) (2003) 367–374.
[17] P. Leone, M. Santarelli, P. Asinari, M. Calì, R. Borchiellini, Journal of Power Sources 177 (1) (2008) 111–122.
[18] A. Lanzini, P. Leone, M. Santarelli, P. Asinari, M. Calì, R. Borchiellini, Journal of Fuel Cell Science and Technology 6 (1) (2009) 0110201–01102014.